SUPPORTING MATERIAL

Beaming of helical light from plasmonic vortices via adiabatically tapered nanotip

Denis Garoli[†1] *, Pierfrancesco Zilio*[†1]*, Yuri Gorodetski*[†2*]*, Francesco Tantussi*[1] *and Francesco De Angelis*[1]

[1] Istituto Italiano di Tecnologia, via Morego 30, I-16163, Genova, Italy.

[2] Mechanical engineering department and Electrical engineering department, Ariel University, Ariel, 407000, Israel

† The authors contributed equally to the present work

* Corresponding author: Prof. Yuri Gorodetski, yurig@ariel.ac.il

Supporting Note 1: Fabrication process of plasmonic vortex lens with central tip.

The method followed to fabricate the samples is based on a procedure introduced and fully described by De Angelis et al. (see ref. 1). The principle relies on FIB-generated secondary-electron lithography in optical resists and allows the preparation of high aspect ratio structure with any 3D profile. The final structure comprises of a 6.2 μm high base-smoothed gold tip on a 150 nm gold layer where *m*-PVL are milled. In order to prepare such a complex architecture a multi-steps fabrication process have been optimized. First of all a 5 / 23 nm Ti / Au bilayer has been deposited, by means of sputtering, on a 100 nm thick Si_3N_4 membrane. On this conductive layer, s1813 optical resist has been spun at 1500 rpm and soft-baked at 90°C for 8 minutes. The resist thickness of 11 μm is achieved by tuning the concentration, spinning time and velocity. On the back of the membrane a thin layer of silver (about 10 nm) is then deposited by means of sputtering in order to ensure the necessary conductibility of the sample for the successive lithographic step. The membranes are then patterned from the backside using a Focused Ion Beam (Helios Nanolab600, FEI company), operated at 30 keV (current aperture: 80pA, dwell time: 500 μs). The tip-like shape has been obtained by patterning successive disks with decreasing diameter and correcting the dose applied for every disk, thus resembling the expected tip profile (**Figure S1(a)**). (To note that the first milled disk present a high thickness (around 80 nm) that will be filled in the successive metallic growth). Due to the high dose of low-energy secondary electrons induced by ion beam / sample interaction, a 30 nm thick layer of resist, surrounding the milled disks, becomes highly cross-linked and insoluble to most solvents. After patterning, the sample is developed in acetone, rinsed in isopropanol and dried under gentle N_2 flow. The back side silver layer has been then removed by means of rapid HNO_3 rinse. At this stage we get a high dielectric tip surrounded by a metallic substrate. Since we need a base-smoothed tip on a 150 nm thick gold layer, an additional layer of metal has been grown of the substrate by means of galvanic deposition (0.12 Amp DC). The galvanic layer is grown up to the tip base so ensuring a very smooth geometry (see **Figure S1(b)**). After the galvanic deposition, a 40 nm thick layer of gold is deposited by sputtering the

sample, tilted 60° with respect to the vertical and rotated, guaranteeing an isotropic coating on both the sidewalls and the base. (In order to avoid any possible direct transmittance from the tips, the back of them has been filled, by means of electron beam induced deposition, with a 200 nm thick layer of platinum). Finally, in order to prepare the sample with the desired *m*-order PVL surrounding the tip, a FIB milling process has been performed on the sample creating the spiral gratings without affecting the quality of metallic tip. Examples of fabricated PVLs are reported in **Figure S1(c)**.

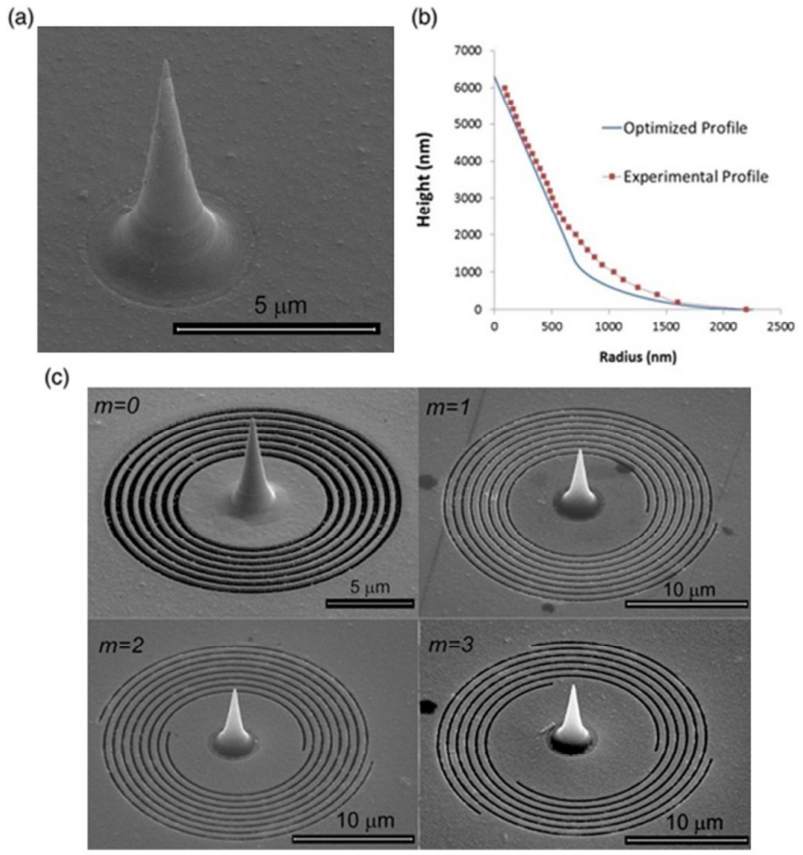

Figure S1. (a) SEM image of an isolated tip. **(b)** Comparison between designed and fabricated profile. **(c)** SEM micrographs of PVLs with topological charge ranging from 0 to 4 and tip at the center.

Supporting note 2: Mode analysis of gold cylindrical waveguides

We report here the analysis of the guided modes of a gold cylindrical waveguide placed along *z*-axis, as a function of the radius, ρ. Their electric field can be expressed as

$$\mathbf{E}_i(r,z) = \tilde{\mathbf{E}}_i(k_{r,i}r)\exp(i\beta z)\exp(il\phi) \quad \text{(S1)}$$

where the subscript i = 1,2 denotes the region outside and inside the cylinder, respectively, β is the complex propagation constant of the mode and $k_{r,i}$ is the transverse wave vector, such that $\varepsilon_i k_0^2 = \beta^2 + k_{r,i}^2$, with $k_0 = \omega / c$ being the vacuum wave vector and ε_1 = 1, ε_2 = -24.1+1.7i the relative permittivities of vacuum and gold at λ = 780 nm.[2] The mode amplitude $\tilde{\mathbf{E}}_i(k_{r,i}r)$ as well as β can be obtained from the solution of Helmholtz equation in cylindrical coordinates in the metal and air domains respectively via imposing the continuity of the tangential components of **E** and **H** fields at the metal surface. The resulting dispersion equation (reported for example in Ref. 3) was solved numerically. In **Figure S2(a,b)** we report respectively the real and imaginary parts of the mode's effective index ($N_{eff} = \beta/k_0$) at λ = 780 nm as a function of the cylinder radius for azimuthal numbers ranging from l = 0 to 7. The inset of **Figure S2(a)** shows the group velocity, v_g, for the first four modes.

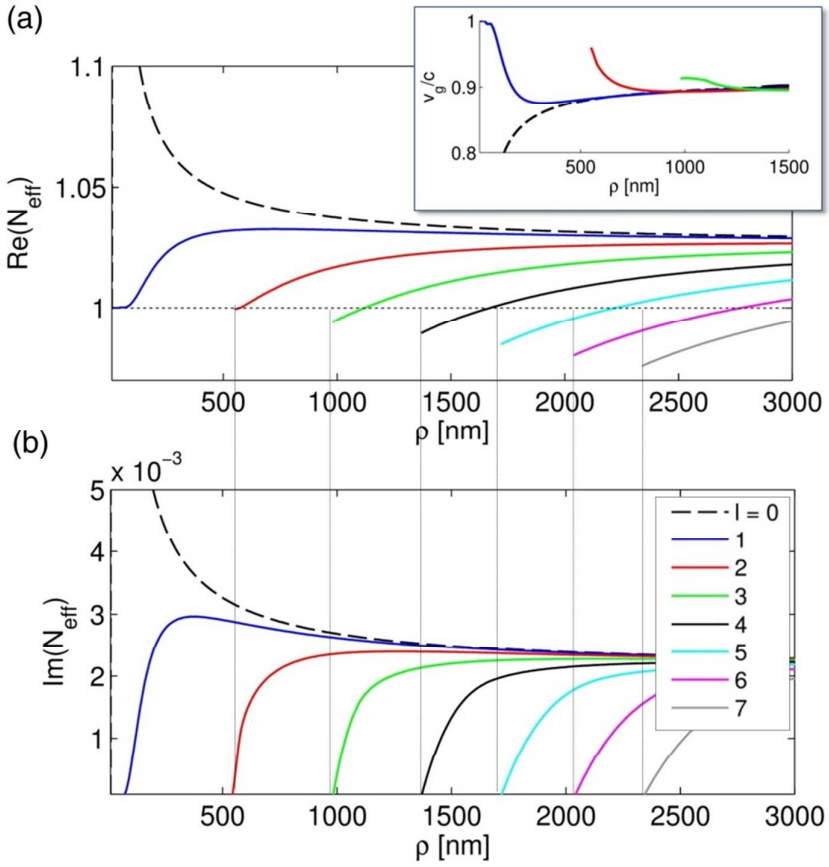

Figure S2. Modal analysis of a cylindrical gold waveguide in vacuum as a function of its radius, ρ, for azimuthal mode index l = 0 to 7 and for a fixed vacuum wavelength λ = 780 nm. **(a)** Real part of the effective mode index, $N_{eff} = \beta/k_0$; inset: normalized group velocity for the first four modes. **(b)** Imaginary part of N_{eff}.

All modes with $l > 1$ exist in a bound form only for ρ larger than some l-dependent cut-off value, at which the modal loss vanishes, Im(β)=0. As can be seen in **Figure S2(a)**, the modes do not cut off exactly at the momentum matching points, namely at $\beta = k_0$ as usually expected from tapered dielectric waveguides.[4,5] The reason of the different behavior in our case is a consequence of the large imaginary part of the modal refractive index, which causes the transverse index k_r in (S1) to become complex-valued.[4,5]

Supporting note 3: Tip optimization studies

In the main text we mention that the tip parameters (curvature radius at the basis, r_c, tip aperture, α, and tip height, h) have been optimized in order to maximize the average tip transmittance (T) and the polarization contrast, Q, for l ranging from 1 to 4. Q is defined as $Q = 1 - P_+/P_-$, with P_+ and P_- being the light powers decoupled by the tip with right and left circular polarization state respectively. In **Figure S3(a-c)** we report the behavior of T and, for convenience, $R = P_+/P_-$, as a function of the various parameters for $l = 1$ ot 4. **Figure S3(d)** reports T and R as a function of l for the optimal parameters set.

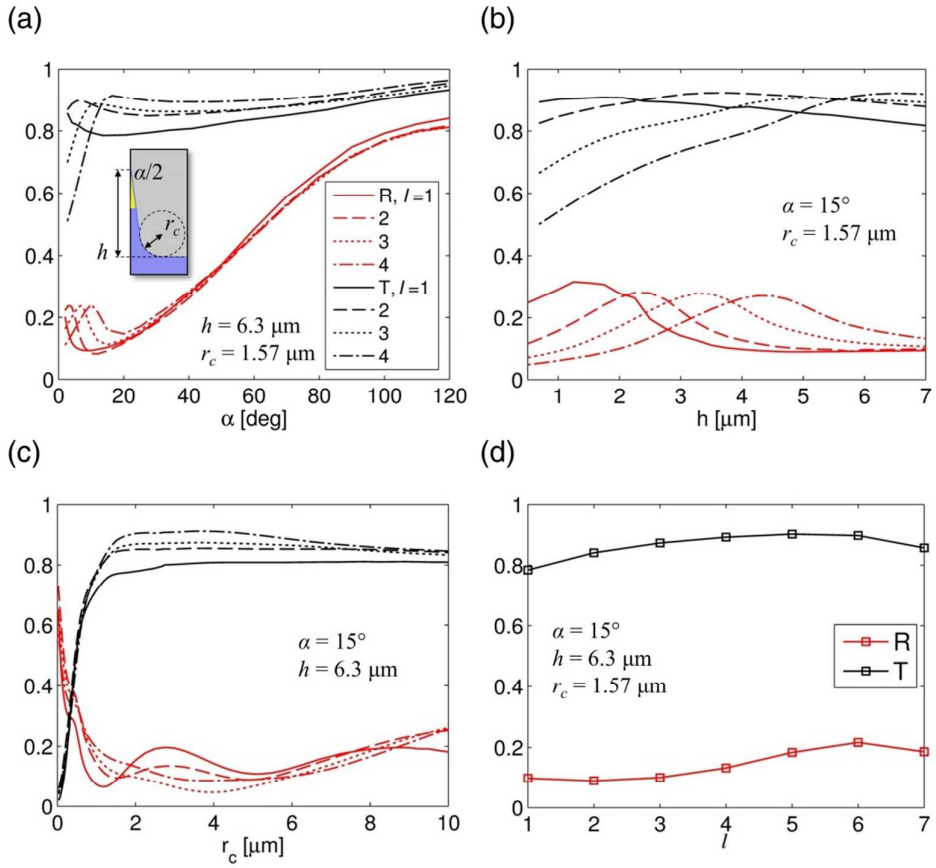

Figure S3. Study of tip transmittance, T, and R parameter (details in the text) as a function of the tip parameters, α **(a)**, h **(b)**, r_c **(c)**, for PV topological charges $l = 1$ to 4. For each plot the remaining parameters are fixed to the optimal. **(d)** R and T as a function of l for the optimized tip.

Supporting References

1. De Angelis, F., Malerba, M., Patrini, M., Miele, E., Das, G., Toma, A., Proietti Zaccaria, R., & Di Fabrizio, E. *Nano Lett*. **13,** 3553–8 (2013).

2. Palik, E. D. *Handbook of Optical Constants of Solids*. (Academic Press, San Diego 1998).

3. Chang, D. E., Sorensen, A. S., Hemmer, P. R. & Lukin, M. D. *Phys. Rev. B* **76,** 035420 (2007).

4. Schmidt, M. a & Russell, P. S. J. *Opt. Express* **16,** 13617–13623 (2008).

5. Spittel, R., Uebel, P., Bartelt, H. & Schmidt, M. A. *Opt. Express* **23,** 12174–12188 (2015).